American Journal of Engineering Research (AJER)
e-ISSN : 2320-0847 p-ISSN : 2320-0936
Volume-02, Issue-11, pp-33-42
www.ajer.org

Research Paper Open Access

Poiseuille Flow in a Vertical Tubular and Porous Membrane for Solar Air Gap Membrane Desalination of Brackish Water.

M. Sene, Y. Mandiang, D. Azilinon
Laboratoire d'Energétique Appliquée (LEA), Ecole Supérieure Polytechnique (ESP) de Dakar, BP 5085
Université Cheikh Anta Diop (UCAD) de Dakar, SENEGAL

Abstract: - Membrane distillation is an emerging technology for desalination that differs from other membrane technologies and in which the driving force for desalination is the difference in vapor pressure of water across the membrane, rather than total pressure. The membrane is hydrophobic material that allows water vapor only to pass across. The vapor pressure gradient is created by heating the source water, thereby elevating its vapor pressure. The major energy requirement is for low-grade solar energy.

The technique used to desalinate water is the Air Gap Membrane Distillation (AGMD), which is more compact, less energy-consuming and required lower temperature (between 40 °C to 80 °C) than conventional distillation processes. In this paper, the work aims to establish a mathematical model of the Navier-Stockes equation applied to a porous membrane of polytetrafluoroethylene. PTFE nanofiber membrane could be used in membrane distillation to produce drinking water from a saline water of NaCl.

Keywords: - *tubular membrane, distillation, brackish water, Poiseuille flow, porous, Darcy's law, Navier-Stockes, desalination*

I. INTRODUCTION

The population of the world is increasing, and fresh water is the primary requirement for life in the universe. However, while water covers about three-quarters of the earth's surface, only 3 % is fresh water from various sources, and not all of this limited quantity is suitable for drinking.

Thus, water treatment is usually needed, and desalination is the most efficient method for providing fresh water from brackish and/or seawater. However, desalination is energy- intensive process. And because of scarce availability of wood and oil and high capital and operational cost, the desalination based on renewable, safe, free and clean solar energy is the promise for a cost-effective solution.

The steady flow in a long channel or in a long tube of circular section under the action the pressure gradient imposed at the two ends, usually known as Poiseuille flow or Hagen Poiseuille flow, is a typical textbook example in fluid dynamics. In the last few years, numerous authors [1-9] have analyzed this problem with the channel geometry when the pressure difference is replaced by a constant external field.

The objective of this work is to analyze theoretically the effect of membrane pore size and porosity.

II. MEMBRANE DISTILLATION CONFIGURATIONS

Membrane distillation (MD) is an emerging technology for desalination. Membrane distillation differs from other membrane technologies, the fact that the driving force for desalination is the difference in vapor pressure of water across the membrane, rather than total pressure. The membranes for MD are hydrophobic, which allows water vapor (but not liquid water) to pass. The vapor pressure gradient is created by heating the source water, thereby elevating its vapor pressure. The major energy requirement is for low-grade thermal energy.

A variety of methods have been employed to impose the vapor pressure difference across the hydrophobic membranes [1]. In every case, the raw water to be desalted directly contacts the hot side of the membrane. The four classes of membrane distillation are therefore (Fig. 1) [2]:

• Direct-Contact Membrane Distillation (DCMD). The cool condensing solution directly contacts the membrane and flows in a countercurrent system to the raw water. This is the simplest configuration. It is well suited for applications such as desalination and concentration of aqueous solutions.
• Air-Gap Membrane Distillation (AGMD) in which an air layer is interposed between the membrane and the condensation surface.
• Sweep-Gas Membrane Distillation (SGMD). A sweep gas pulls the water vapor and/or volatilizes from the system. Useful when volatile salts can be removed from an aqueous solution.
• Vacuum Membrane Distillation (VMD). A vacuum is used to pull the water vapor out of the system. Useful when volatile salts can be removed from an aqueous solution.
Membranes with lower thermal conductivities and higher porosities improve the performance of single-membrane designs while thinner membranes improve the performance of air-gap designs. This device can be used with a solar heating system which already uses concentrated salt solutions.

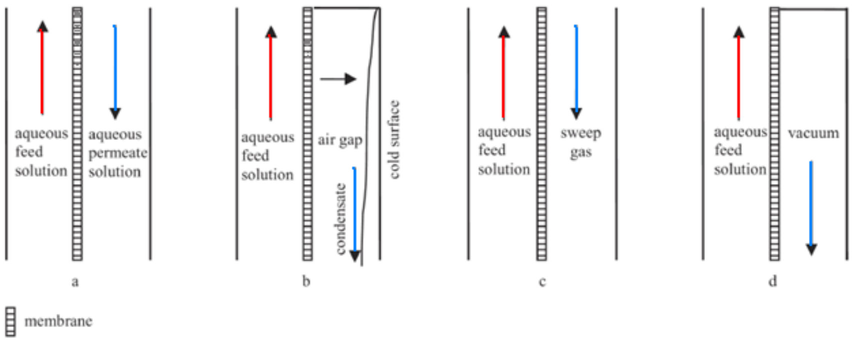

Figure 1 - Membrane distillation configurations (a) DCMD, (b) AGMD, (c) SGMG, and (d) VMD

The advantages of membrane distillation are:
• It produces high-quality distillate.
• Water can be distilled at relatively low temperatures (40 °C to 90 °C).
• Low-grade heat (solar, industrial waste heat or desalination waste heat) may be used.
• The water does not require extensive pretreatment as in pressure-based membrane treatment.

III. PHENOMENA DESCRIPTION OF AGMD

Out of all the different MD processes, AGMD was selected for modeling because the model was more general than for some other MD processes, and is therefore easier to modify for modeling other types of MD processes. A schematic of an air-gap membrane distillation unit is shown in figure 2. The brackish or saline water to be distilled is heated and passed by one side of the membrane. Water vapor diffuses across the membrane and air gap to the other side, where it condenses on the cooler surface. The right side of the air gap is kept cool by a flow of cooling water. The overall process is driven by a gradient in water vapor pressure, rather than a difference in total pressure. Thermal energy is required to elevate the vapor pressure of water in the hot stream. Figure 3 illustrates the scheme of a cylindered membrane PTFE.

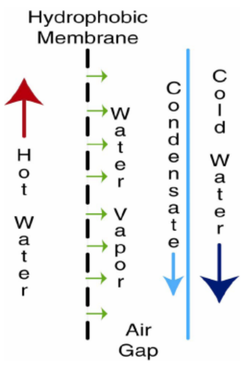

Figure 2 - Schematic of air-gap membrane distillation.

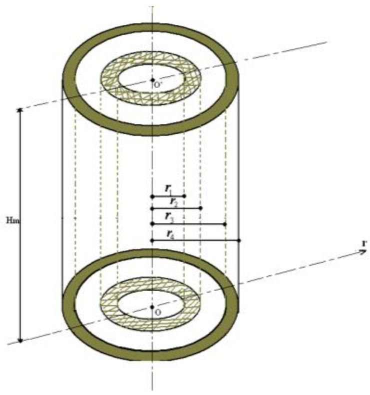

Figure 3 - Vertical and cylindered membrane PTFE

The membrane itself is hydrophobic with pore sizes r_p, usually in the range of 0.05 µm to 0.2 µm. Lawson and Lloyd (1997) [3], for example, used polypropylene membranes with maximum pore sizes r_p ranging from 0.3 µm to 1.1 µm. Water is kept from penetrating the pores by surface tension and capillary pressure. Table 1 summarizes surface energy of some membrane materials and table 2 recapitulates characteristics of commercial materials commonly used in membrane distillation.

Table 1 - Experimental surface energy of some material membranes used in MD [4]

Membrane materials	Surface tension γ_{LV} (N/m)
PTFE	0.0191
PP	0.0300
PVDF	0.0303
PE	0.0332

Table 2- Characteristics commercial materials commonly used in membrane distillation **[5]**

Membrane Trade Name	Manufacturer	Material	Thickness (μm)	pore size y (μm)	Conductivities k ($W^{-1}K^{-1}$)	Porosity ε (%)
TF200	Gelman	PTFE	55	0.20	0.0382	75-85
TF450	Gelman	PTFE/PP	178	0.45		80
TF1000	Sartorious	PTFE		1.00		75-80
GVHP	Millipore	PVDF	118	0.22	0.041	70
HVHP	Millipore	PVDF	140	0.45	0.040	75
S6/MD020CP2N	Akzo Nobel Microdyn	PP	450	0.2		70

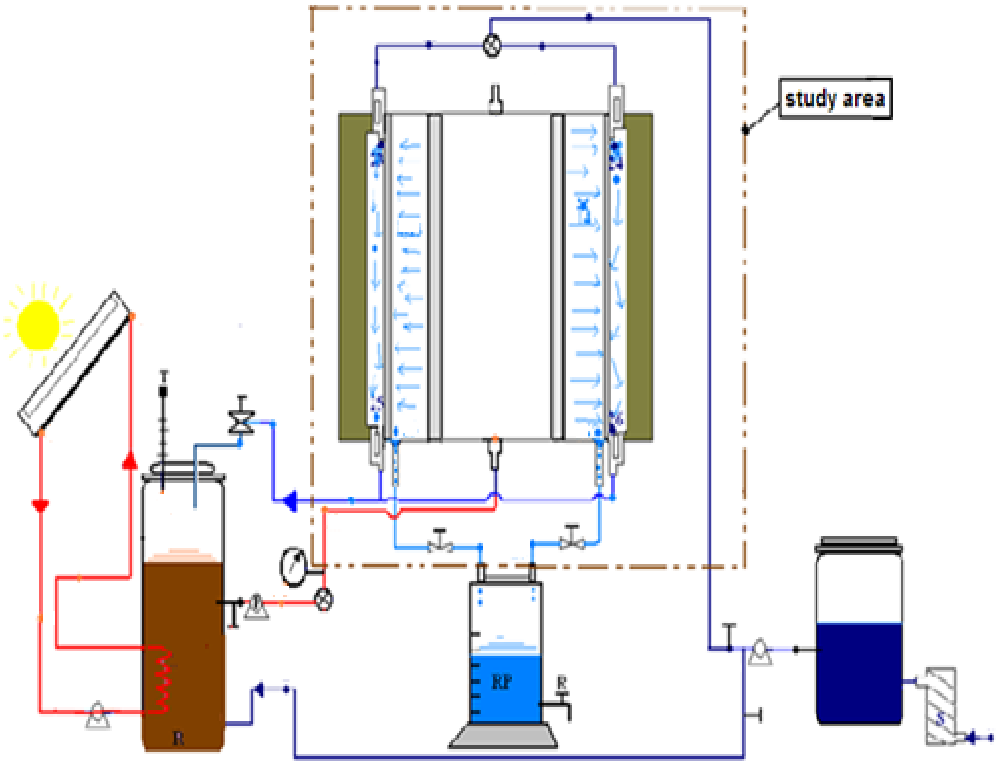

Figure 4 - Scheme of an operating modular solar system of the membrane distillation

To study the performance of the modular solar thermal desalination system, analytical calculations have been made as illustrated (Fig.4). The salt-water supply is heated from a set (solar collector (7-8), conventional heat exchanger (5-6)). In the tubular porous membrane, the temperature of the brine is between 30 °C and 90 °C [**4**]. The wall of the tube is hydrophobic allowing only radial diffusion of the vapor. Steam generated through the membrane and the air gap condenses on the inner wall of the second pipe to be collected. The energy balance equations will be presented in next sections.

IV. THE POISEUILLE MODEL FLOW: THEORETICAL APPROACH

The Poiseuille flow model is based on viscous flow through a cylindrical capillary wall (Fig.5). When the capillary diameter is large compared with mean free path lengths and a pure substance is present in the capillary we have the classical Poiseuille's problem.

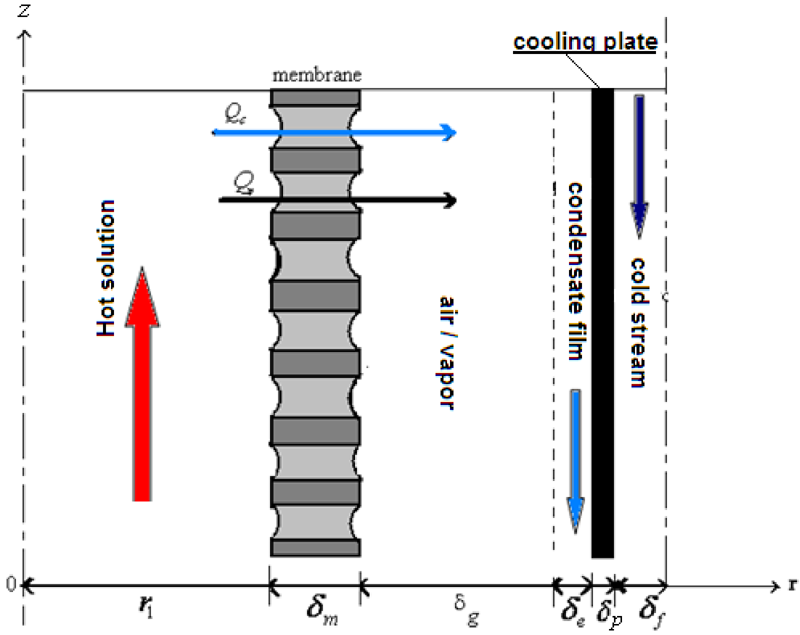

Figure 5- AGMD cell configurations

4.1. Mathematical and physical modeling at steady state

A steady state, laminar, incompressible, viscous and isothermal flow in a cylindrical tube with a permeable wall is considered. The velocity profile in laminar flow in a tubular membrane is plotted as illustrated (Fig.6).

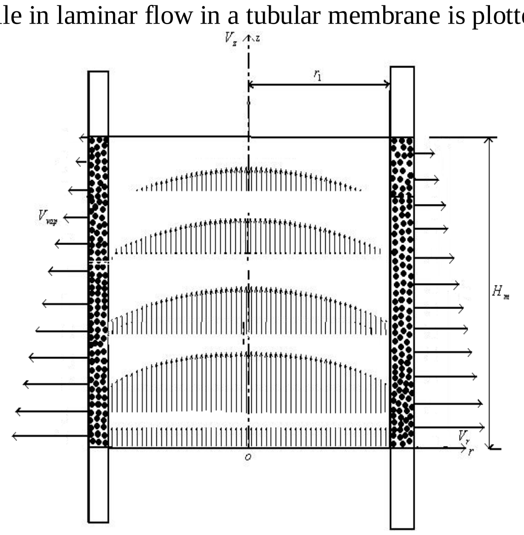

Figure 6 - Plot of velocity profile for laminar flow in a tubular membrane

For micro porous membrane, the viscous flow equation may be written as:

$$J_v = \dot{m}_p n_p \tag{1}$$

where

$$n_P = \frac{1}{\pi} \frac{\varepsilon}{r_p^2} \tag{2}$$

assuming the pore is a uniform circular tube.

Balancing the viscous shear forces acting over the surface, the velocity distribution over the cross section of the pore is given by:

$$V_{(r)} = \frac{r^2 - r_p^2}{4\mu}\frac{\partial p}{\partial r} \tag{3}$$

The mass flow rate through the pore can be obtained by integrating equation (3) over the cross section of the pore size.

$$\dot{m}_p = \frac{\pi}{8}\frac{r_p^4}{\delta_m}\frac{\rho_v}{\mu_v} \tag{4}$$

Substituting equation (4) and (2) into (1) we have

$$J_v = \frac{1}{8}\frac{r_p^2 \varepsilon}{\delta_m \tau}\frac{\overline{p}}{R\overline{T}}\frac{M_v}{\mu_v}\Delta p_v \tag{5}$$

where T_{hm} and T_{cm} are the temperatures of the hot and cold sides of the membrane.
And in general, equation (5) may be written as:

$$J_v = K_p . p_v \tag{6}$$

where K_p, the permeability of the membrane due to Poiseuille flow, is expressed by

$$K_p = \frac{1}{8}\frac{r_p^2 \varepsilon}{\delta_m \tau}\frac{\overline{p}}{R\overline{T}}\frac{M_v}{\mu_v} \tag{7}$$

The vapor pressure (p_v) were calculated using the Antoine equation [1] as

$$ln\, p_v = 23.328 - \frac{3841}{T - 45} \tag{8}$$

The effect of the presence of salt in the solution on the vapor pressure at the hot surface onto the membrane side has been accounted by using the empirical correlation for the boiling point elevation. Raoul's Law can be used to express the vapor pressure at the hot side of the membrane (p_{hm}) as

$$p_{hm} = (1 - C_{s,hm}) p_v (T_{hm}) \tag{9}$$

4.2. Velocity problem

Consideration is given to a constant property fluid flowing in a straight tube of circular cross section, at the walls of which there is a uniform mass transfer.

The mass conservation and momentum equations, Navier-Stokes equations expressed in cylindered coordinates with axisymetric assumption are:

$$\rho\left(V_r \frac{\partial V_r}{\partial r} + V_z \frac{\partial V_r}{\partial z}\right) = -\frac{\partial P}{\partial r} + \mu\left[\frac{\partial}{\partial r}\left(\frac{1}{r}\frac{\partial}{\partial r}(rV_r)\right) + \frac{\partial^2 V_r}{\partial z^2}\right] \tag{10}$$

$$\rho\left(V_z \frac{\partial V_z}{\partial z} + V_r \frac{\partial V_z}{\partial \overline{r}}\right) = -\frac{\partial P}{\partial z} - \rho g + \mu\left[\frac{1}{r}\frac{\partial}{\partial r}(rV_z) + \frac{\partial^2 V_z}{\partial z^2}\right] \tag{11}$$

where V_r and V_z are the velocity components.

At the permeable, porous, homogeneous and isotropic wall, the wall suction velocity is given by Darcy's law as mentioned in the previous section. Considering the boundary conditions, at the inlet developed laminar profile is considered, ie, Poiseuille flow which leads to:

$$V_z = 2V_e\left[1 - \left(\frac{r}{r_1}\right)^2\right]\exp\left[-4\sqrt{\frac{J_v r_1}{\mu}}\left(\frac{z}{r_1}\right)\right] \tag{12}$$

$$V_r = 4V_e\sqrt{\frac{J_v r_1}{\mu}}\left[\left(\frac{r}{r_1}\right)^2 - \frac{1}{2}\left(\frac{r}{r_1}\right)^4\right]\exp\left[-4\sqrt{\frac{J_v r_1}{\mu}}\left(\frac{z}{r_1}\right)\right] \tag{13}$$

In the entrance region the flow is not developed, and the following equation has been recommended for turbulent flow in tubes. The solution depends on both the Reynolds axial and filtration number.

$$N_u = 0.097 R_e^{0.73} . P_r^{0.13} \quad \text{laminar flow} \qquad (14)$$

$$N_u = 0.036 R_e^{0.96} . P_r^{\frac{1}{3}} \left(\frac{D}{L}\right)^{0.055} \quad \text{for} \quad 10 \le \frac{L}{D} \le 400 \quad \text{turbulent flow} \qquad (15)$$

where D is the equivalent diameter of the flow channel and L is the tube length

$$Pr = \frac{\mu C_p}{\lambda} \quad \text{Prandtl number}$$

$$Re_{r1} = \frac{\rho V_e r_1}{\mu} \quad \text{Reynolds number}$$

V. RESULTS AND DISCUSSIONS

Simulations have been carried out for following data:

- the analysis is made for the inlet temperature of the feed solution (T_{hi}) in the range (40 to 80) °C computed at 5 °C increments;
- Steady state: feed solution inlet velocities (V_e) of 0.1 $m.s^{-1}$ to 0.8 $m.s^{-1}$;
- cooling solution inlet temperatures (Tci) of 5 °C to 20 °C at 5 °C increments;
- air/vapor gap widths (δg) of 1 mm to 5 mm at 1 mm increments;
-membrane thermal conductivities (k_m) of (0.05 to 0.3) $Wm^{-1}.K^{-1}$ at 0.05 $Wm^{-1}.K^{-1}$ increments;
- membrane porosities (ε = 0.70 to 0.80);
-membrane tortuosity (τ = 1.7).

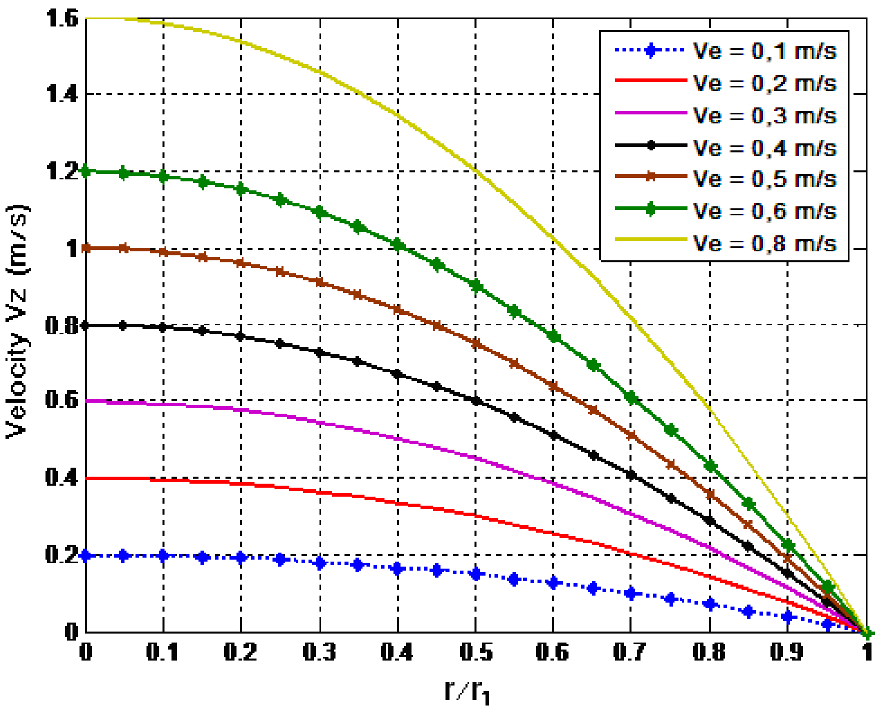

Figure 7 - Plot of velocity along the membrane length

It is observed (Fig.7) the boundary layer grows with a faster rate near-by the entrance of the channels. This implies that the heat transfer coefficient, and thus the local permeate flux, are (as expected) higher near-by the hot channel entrance.

The velocity increases along the radius of the membrane with the input speed of the hot solutions (0.1 m/s to 0.8 m/s). We observe that (Fig.8) it is higher in the wall of the membrane, which allows a relatively large water production. This effect can reduce the resistance time of the steam within the membrane. The velocity affects the process by reducing the boundary layer thicknesses of the temperature and concentration of the hot solution and the temperature of the cold solution.

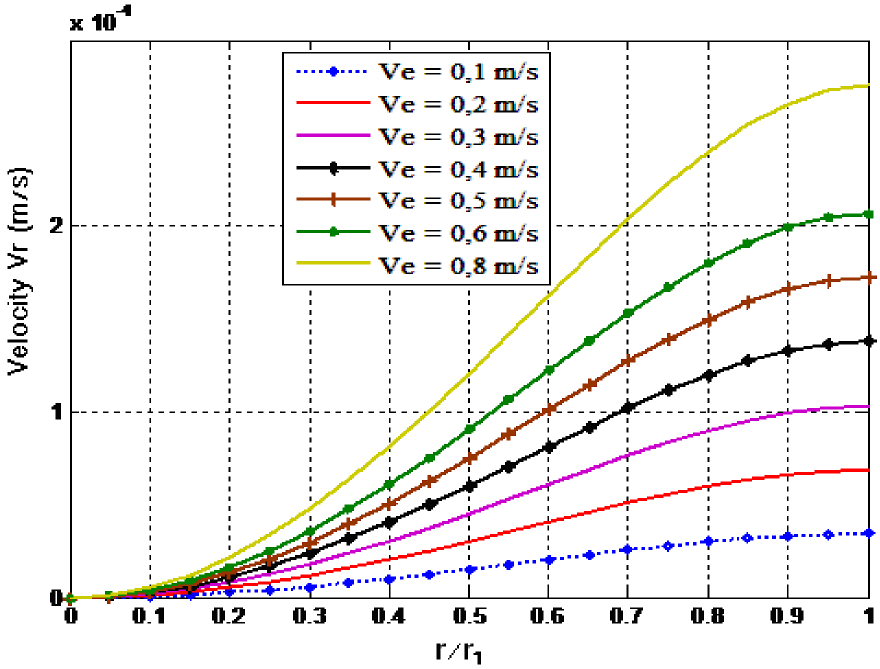

Figure 8 - Plot of velocity through the radial axis

The feed solution temperature has a major effect on the permeate flux. This increase is larger at higher temperatures because the vapor pressure increases exponentially with increasing temperature.
Figure 9 shows the permeate flux (J) as a function of both the hot and the cold solutions inlet velocities. The improvement is because higher velocities reduce the z-direction temperature drop in the solutions, increasing the driving temperature difference, and that has a higher effect on the vapor pressure in the hot solution.

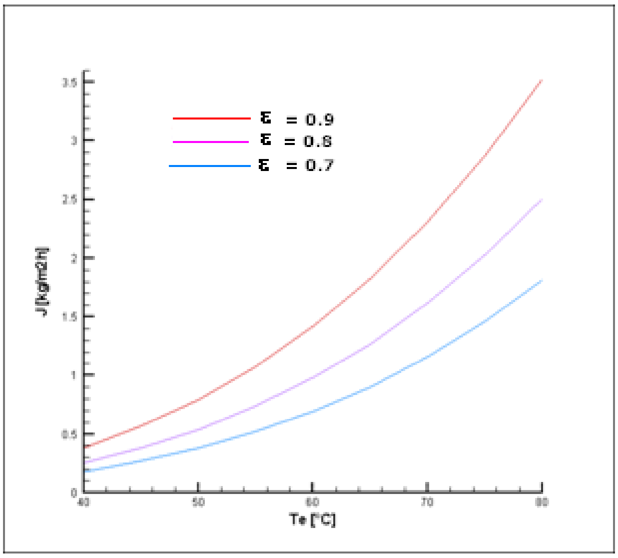

Figure 9 - Effect of the average temperature of feed and permeate side solution of the commercial. PTFE membranes [T_{ci} = 20 °C, u_{hi} = 0.1 m.s^{-1} , ε = 0.7 to 0.9].

Figure 10 shows that the permeate flux from the interior of the membrane increases as a function of porosity. Depending on the value of dimensionless radius it decreases slightly, indicating that the appearance of the membrane permeable and selective.

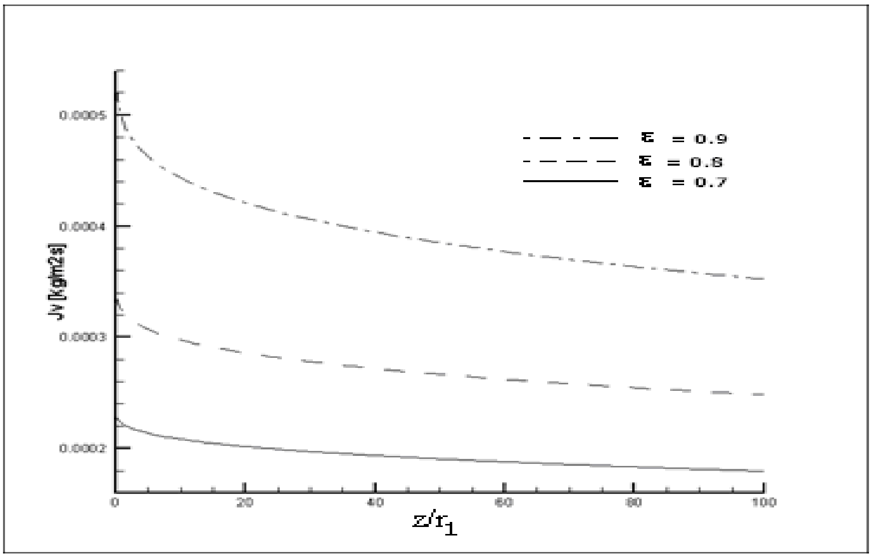

Figure 10 - The effect of membrane radius on the permeate flux.

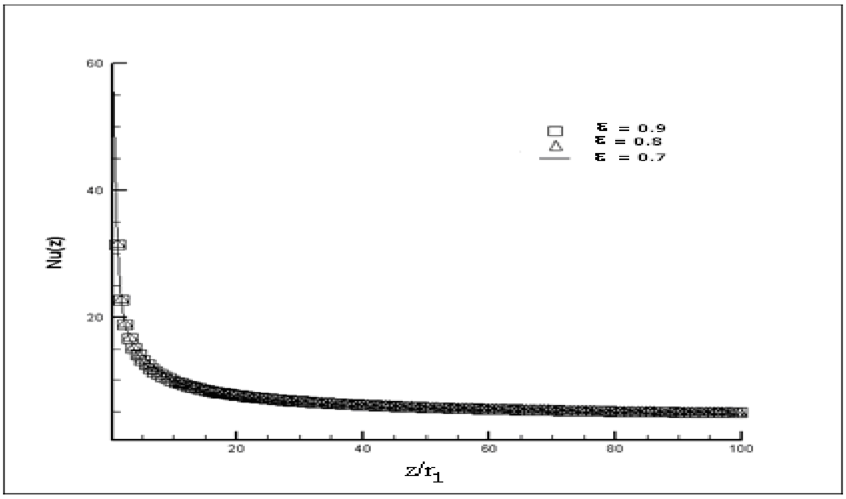

Figure 11 - The effect of distance on the Nusselt number.

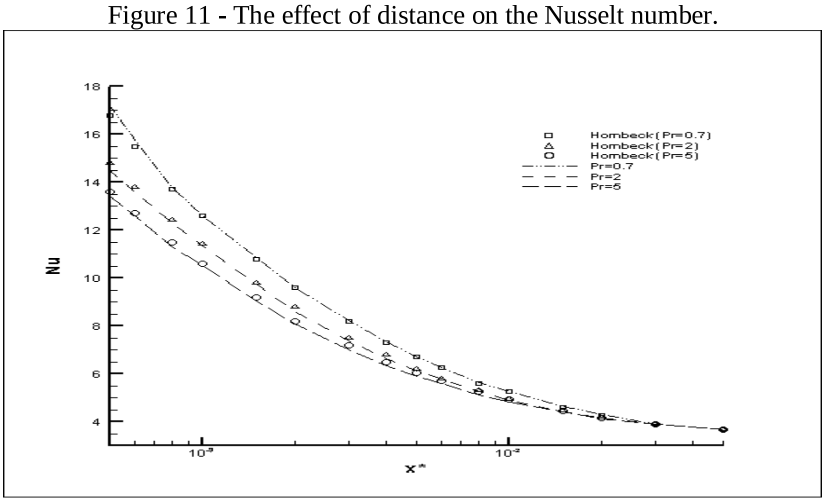

Figure 12 - Hombeck solution in comparison to our model

To validate our model, we compared it with the experimental work of Hombeck (Fig.12). The Nusselt number characterizes energy heat transfer between a solid surface and a fluid in motion. The Prandlt number compares the speed of the thermal and hydrodynamic phenomena in a fluid. A high Prandlt (Pr = 5) indicates that the temperature profile.

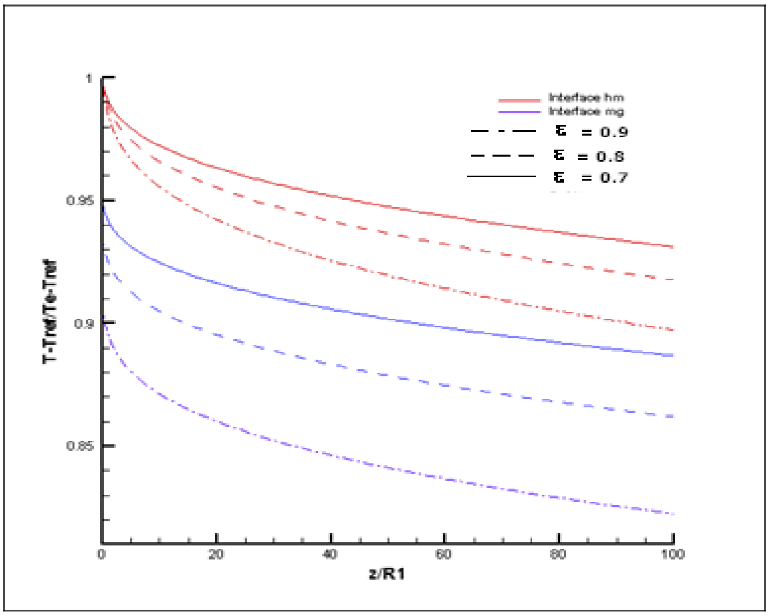

Figure 13 - Effect of polarization of temperature

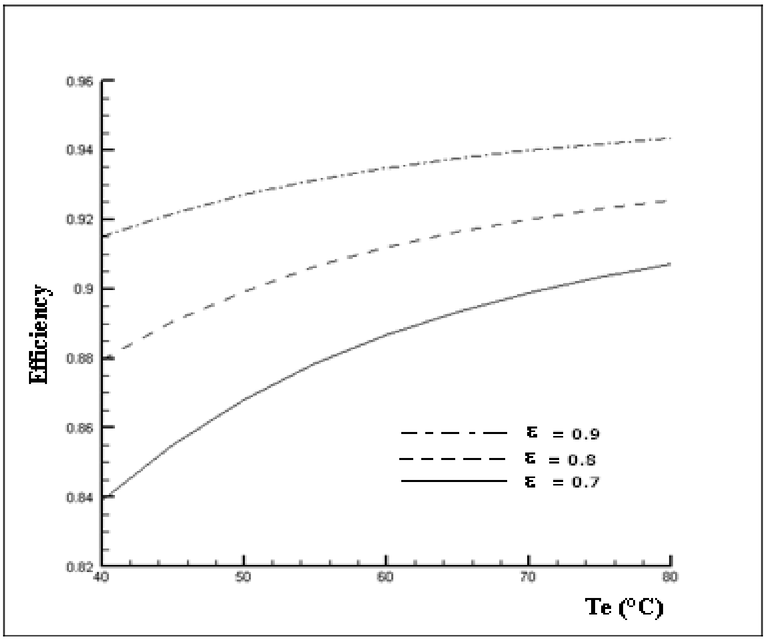

Figure 14 - Efficiency of the AGMD model

The performance of the proposed model is the order of 0.94 % for different porosities (0.7, 0.8 and 0.9) on this curve, it increases with the operating temperature of the system that is to say from 40 °C to 80 °C.

VI. CONCLUSIONS

This paper describes Poiseuille flow model to simulate the permeate flux of water in cross flow filtration tubular membrane. The flow in the hot fluid region and in the porous medium is described by the Navier-Stokes equations and Darcy's law. First the model was carefully validated by Hombeck experimental model.

The effectiveness and efficiency of the model have been assessed, however, understanding of the physical phenomena and the behavior of the model should require the pursuit and deepening of this work.

But we think that Poiseuille flow should not be neglected in the process of desalination since it intervenes largely depending on the type of membrane used.

VII. LIST OF SYMBOLS

C_s mole fraction of NaCl
d_h half-width of the flow channel, m
g acceleration of gravity, m.s^{-2}
H_m membrane length, m
J length-averaged permeate flux at the hot side of the membrane, kg.m^{-2}.s^{-1}
K membrane Permeability, m^{-1}.s
J_v local permeate flux at the hot side of membrane, in vapor phase, kg.m^{-2}.s^{-1}
K_m mass transfer coefficient, J.m^{-2}.s^{-1}.K^{-1}
M molar mass, kg.mol^{-1}
m mass, kg
$\dot{m}$ mass flow rate, kg.s^{-1}
Nu Nusselt number
P pressure, Pa
Pr Prandlt number
P_v water vapor pressure, Pa
R_e Reynolds number of the hot solution channel
R Universal gas constant, J.kmol^{-1}.K
r_p membrane pore size, m
r_1 largest membrane pore , m
T temperature, ^{o}C
T_{ci} inlet temperature of cold solution, ^{o}C
T_{hi} inlet temperature of hot solution, ^{o}C
$\bar{T}$ Average temperature, ^{o}C
V velocity, m.s^{-1}
V_e velocity of feed solution, m.s^{-1}
Vr the velocity in radius direction, m.s^{-1}
r coordinate normal to the solution flow
z coordinate along the solution flow

Greek letters

ΔP water vapor pressure difference, Pa
δ Thickness or width, m
ε porosity of the membrane
γ_l surface tension of water, N.m^{-1}
µ dynamic viscosity, kg.m^{-1}.s^{-1}
ρ density, kg.m^{-3}
τ tortuosity

Subscripts

a Air
atm Atmosphere
Avg Average
c cold solution
f condensate film
fp condensate film/cooling plate interface
g vapor/air gap
gf air gap/condensate film interface
h hot solution
hi inlet of the hot channel
hm hot liquid/membrane interface
i inlet of the channel or ith domain
m membrane
mc membrane cold side
mg membrane/air gap interface

REFERENCES

[1] L. MARTINEZ, F.J.FLORIDO-DIAZ, A.HERNANDEZ, P. PRADANOS « *Characterisation of three hydrophobic porous membranes used in membrane distillation: Modelling and evaluation of their water vapour permeabilities* » - Journal of membrane science 203 (2003) 15-27.

[2] A.EL-ABASSI, A.HAFIDI, M.C.GARCIA-PAYO, M. KHAYET "*Concentration of olive mill wastewater by membrane distillation for polyphenols recovery*",- Semlalia, Marrakech, Morroco, February 2009.

[3] K. CHARFI , M. KHAYET, M.J. SAFI , "*Numerical simulation and experimental studies on heat and mass transfer using sweeping gas membrane distillation*", - 28040 Madrid, Spain

[4] M.SENE, « *Transferts de chaleur et de masse dans des procédés de dessalement par distillation membranaire, type AGMD - valorisation des ressources en eau dans le delta du saloum* ». - Thèse de doctorat, Université Cheikh Anta Diop de Dakar Sénégal (2010).

[5] 5.J. PHATTANARAWIK, R JIRARATANANON, A.G.FANE, « *Effect of pore size distribution and air flux on mass transport in direct contact membrane distillation*» - Toogkru, Bangkok, Thailand, 2002

[6] JULIÁN BLANCO GÁLVEZA, LOURDES GARCÍA-RODRÍGUEZ, ISABEL MARTÍN-MATEOS, "*Seawater desalination by an innovative solar-powered membrane distillation system: the MEDESOL project*", - Tabernas, Almería, Spain

[7] E. MATHIOULAKIS, V. BELESSIOTIS, E. DELYANNIS, "*Desalination by using alternative energy:Review and state-of-the-art*", - Aghia Paraskevi, 153-10, Athens, Greece

[8] HAZIM MOHAMEED QIBLAWEY, FAWZI BANAT, "*Solar thermal desalination technologies*", 22110 Irbid, Jordan

[9] S. MIDDLMANN « *An introduction to fluid dynamics : principles of analysis and design* » - University of California, San Diego pp 261-267.

[10] K. DAMAK, A. AYADI, B. ZEGHMATI, P. SCHMITH, « *A new Navier-Stokes and Darcy's law combined model for fluid flow in crossflow filtration tubular membranes* » - Laboratoire Radio Analyse et Environnement, Ecole nationale d'ingénieurs de Sfax, TunisieDesalination 161 (2004) 67-77.

[11] M.S. El-BOURAWI, Z. DING, R. MA, M. KHAYET, « *A framework for better understanding membrane distillation separation process* », - State Key Laboratory of Chemical Resource Engineering, Beijing University of Chemical Technology, Beijing 100029, PR China , Journal of Membrane Science 285 (2006) 4-29.

[12] A.M. ALKAIBI, N. LIOR, « *Transport analysis of air gap membrane distillation* » - Department of Mechanical engineering and Applied of Pennsylvania, USA. Journal of Membrane Science 255 (2005) 239-253.